

LARGE AREA TOPCON CELLS REALIZED BY A PECVD TUBE PROCESS

Frank Feldmann¹, Tobias Fellmeth¹, Bernd Steinhauser¹, Henning Nagel¹, Daniel Ourinson¹, Sebastian Mack¹, Elmar Lohmüller¹, Jana Polzin^{1,2}, Jan Benick¹, Armin Richter¹, Ana Moldovan¹, Martin Bivour¹, Florian Clement¹, Jochen Rentsch¹, Martin Hermle¹, Stefan W. Glunz^{1,2}

¹Fraunhofer Institute for Solar Energy Systems ISE, Heidenhofstraße 2, 79110 Freiburg, Germany

²INATECH, University of Freiburg, Emmy-Noether-Straße 2, 79110 Freiburg, Germany

ABSTRACT: TOPCon is an appealing choice for next-generation solar cells as it minimizes surface recombination, enables low contact resistivities, and provides high thermal stability thereby rendering it compatible with screen-printed metallization. While TOPCon is commonly realized by low-pressure chemical vapor deposition (LPCVD), this paper discusses the use of a plasma-enhanced chemical vapor deposition (PECVD) tool, which are commonly used for deposition of SiN_x or AlO_x. It will be shown that thick screen-printing compatible TOPCon layers providing excellent surface passivation can be realized with such tool. Additionally, the firing stability of TOPCon/SiN_x stack will be discussed and first solar cell results will be presented. The IV parameters of the best solar cell were: $V_{oc} = 691.2$ mV, $FF = 80.7\%$, $J_{sc} = 40.4$ mA/cm², and $\eta = 22.5\%$.

Keywords: PECVD, Passivation, Solar Cell, Silicon

1 INTRODUCTION

Passivating contacts realized by a thin interfacial oxide and a heavily-doped poly-Si layer (hereafter referred to as TOPCon) are considered a follow-up technology of PERC cells. Its huge efficiency potential has been underlined by both an IBC lab cell achieving 26.1% efficiency [1] and a 25.8%-efficient n-type lab cell featuring front and rear contacts [2]. To date, research institutes and manufacturers are working towards the implementation of TOPCon into a lean solar cell process flow which makes use of well-established PV manufacturing processes such as diffusion, PECVD, and screen-printing. The upscaling of the n-type TOPCon cell featuring a boron-diffused emitter and TOPCon rear contact [3] has attracted considerable attention and is being researched by major cell manufacturers. In 2016 Stodolny et al. reported the first cell made with industrial manufacturing tools having an efficiency of 20.7% [4]. Since then the efficiency has climbed to 22.8% [5] and even 23.6% [6] within the last three years. Such progress was i.a. strongly supported by progress in metallization paste development for the contacting of both boron emitter and TOPCon. For instance, $J_{0,met}$ values of 35 fA/cm² (200 nm poly-Si) [7] and 100-200 fA/cm² (100 nm poly-Si) [8] were reported.

Recently, Chen et al. reported on the successful retrofitting and upgrading of an old Al-BSF production line enabling mass manufacturing of industrial TOPCon (i-TOPCon) solar cells with median efficiency of 23% [6]. The authors' work impressively highlights the potential of the TOPCon technology. The authors, however, remarked that the current cell process needs further simplification and optimization. Most commonly such process sequence utilizes low-pressure chemical vapor deposition (LPCVD) tools for realization of TOPCon. This technology enables in-situ formation of the tunnel oxide and ensures conformal deposition of a-Si or poly-Si layers. However, the deposition rate and the crystallinity of the film strongly depend on the deposition temperature. Furthermore, the deposition rate is strongly enhanced upon addition of diborane (B₂H₆) and slightly reduced by phosphine (PH₃), respectively. Therefore, precise temperature control and a highly uniform distribution of the precursor gases are vital to ensure a reproducible and homogeneous deposition process. Another challenge that is introduced by the conformity of

the layer deposition is that due to the wrap around always an additional masking as well as etching step is required. An appealing alternative is PECVD as it is usually regarded as a single-sided deposition technique but a minimal wrap-around at the cells' edges can occur. One challenge with PECVD films is the risk of blistering due to large amounts of hydrogen incorporated within the Si layer thereby, possibly, putting restrictions on the maximum film thickness.

In this work, we report on the use of a centrotherm c.PLASMA 2000 PECVD tool, which is commonly used to deposited dielectrics, e.g. SiN_x or AlO_x. In an early report we have already demonstrated that thin a-Si layers can be softly deposited onto a thin interfacial oxide by such tool [9]. Here, we will discuss the deposition of thick layers using an industrial-viable boat configuration. Furthermore, we will address the firing stability of our TOPCon layers. Finally, first solar cell results will be presented and analyzed with emphasis on recombination-induced losses.

2 TOPCON PECVD DEPOSITION

Symmetrical lifetime samples were prepared on M2-sized, n-type Cz wafers. After saw damage removal, the wafers were cleaned following the RCA procedure. Thereafter, an about 1.2 nm thin tunnel oxide layer was thermally grown in a tube furnace. In-situ Phosphorus-doped a-Si films were deposited by PECVD using a vertical boat configuration with 144 slots which closely resembles the industrial standard. The samples received a 10-minute anneal at 900°C and hydrogenation was carried out by depositing Al₂O₃ by spatial ALD and subsequent forming gas annealing at 425°C.

Fig. 1a plots the a-Si film thickness over the wafer position in the boat. Column A refers to a position close to the gas inlet, while column F refers to a position close to the gas outlet. The front side, which was first deposited onto, showed 10 to 20 nm larger film thickness as the rear side. This is a well-known phenomenon of tube PECVD systems and can be remedied by adjusting plasma power or deposition time. A small gradient in film thickness along the boat can be observed. This is the result of depletion of precursor gases near the gas outlet and will be tackled during process optimization in the near future. Fig. 1b shows the implied open-circuit voltage (iV_{oc}) measured after annealing and subsequent

hydrogen passivation. After annealing iV_{oc} was in the range of 690 mV to 710 mV and was increased to 740 mV by hydrogenation. The observed gradient in iV_{oc} measured after annealing is likely attributed to some depletion of phosphine near the gas outlet and is not the result of the lower film thickness. However, these subtle differences were leveled out by the hydrogenation process.

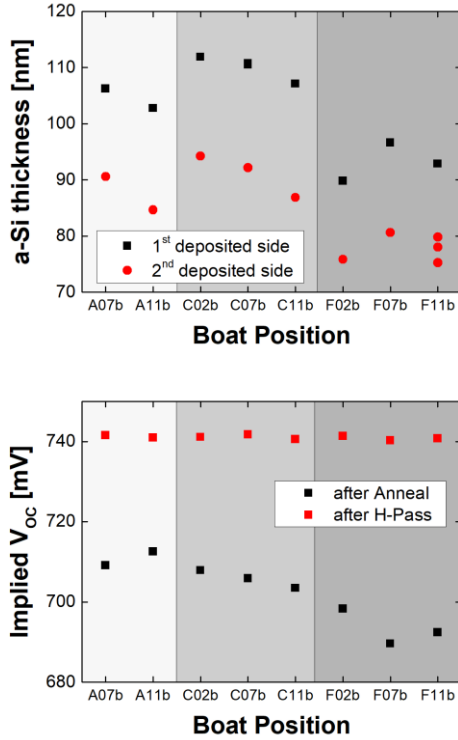


Figure 1: a) a-Si film thickness and b) iV_{oc} values before and after hydrogenation plotted against wafer position in a vertical PECVD boat.

3 TOPCon SOLAR CELLS

3.1 Experimental Details

TOPCon solar cells were realized on M2-sized, n-type 4 Ω cm wafers. After texturing, the wafers received a tabula rasa process at 1050°C for 80 min in order to dissolve oxygen precipitates in the wafer. A low-pressure BBr₃ diffusion furnace was used to realize the emitter. The latter exhibited a mean sheet resistance (R_{sheet}) of 122 Ω /sq and the standard deviation within this batch was no more than 4%. Following wet-chemical rear side emitter removal, TOPCon featuring 100 nm or 170 nm poly-Si was realized following the processes described above. Due to the single-sided nature of the PECVD process, the wet-chemical process to remove any poly-Si at the front – as described by Chen et al – could be omitted. Nevertheless, a wet-chemical clean (at least an HF-dip) was conducted to remove any surface oxide before deposition of 6 nm Al₂O₃ at the front side by spatial ALD. After outgassing, 70 nm SiN_x:H were deposited on either side by PECVD. A busbar-less metal grid was screen-printed using dedicated AgAl and Ag pastes and fired in an industrial conveyor belt furnace at peak temperatures near 760°C. The cells were measured using a Halm inline flash tester which is equipped with a Pasan GridTouch unit featuring a black chuck.

Half-fabricates were processed in parallel in order to

determine both the surface passivation after firing and the recombination prefactor at the metal contacts ($J_{0,met}$) by means of QSSPC-calibrated photoluminescence imaging (PLi) [10]. The contact resistivity, ρ_c , was determined from the transfer length method (TLM) after the wafers had been diced into stripes.

3.2 Surface Passivation and Recombination at Metal Contacts

The surface passivation of TOPCon was investigated using single-side textured wafers featuring a TOPCon/SiN_x:H layer stack on both sides. The effect of firing was compared to a low temperature hydrogenation process (forming gas anneal at 425°C). The lifetime characteristics are plotted in Fig. 2 and clearly show that firing deteriorates the surface passivation of TOPCon compared to the low-temperature hydrogenation process. The corresponding iV_{oc} values were about 700 mV after firing. Interestingly, the surface passivation could be recovered by applying an additional forming gas anneal. Since then work has been dedicated to the firing stability of TOPCon and after process optimization an excellent surface passivation was achieved after firing. The resulting lifetime characteristic is depicted in Fig. 3 and the corresponding iV_{oc} value was about 735 mV.

The surface passivation of the boron-doped emitter was determined on symmetrically diffused and passivated samples and J_{0e} took a value in the range of 25-40 fA/cm². For optimum firing conditions a $J_{0,met}/\rho_c$ pair of 600-700 fA/cm² and 3 m Ω cm² was obtained, while the former value presents an improvement by a factor of 4-5 compared to previous work [11].

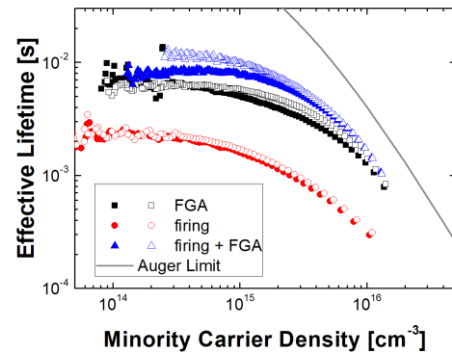


Figure 2: Lifetime characteristics of symmetrical lifetime samples passivated by TOPCon after forming gas anneal and firing, respectively.

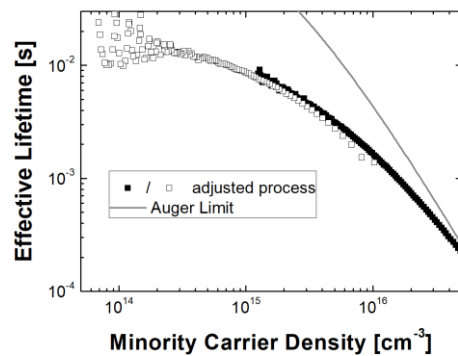


Figure 3: Lifetime characteristics of samples passivated by TOPCon measured after process optimization.

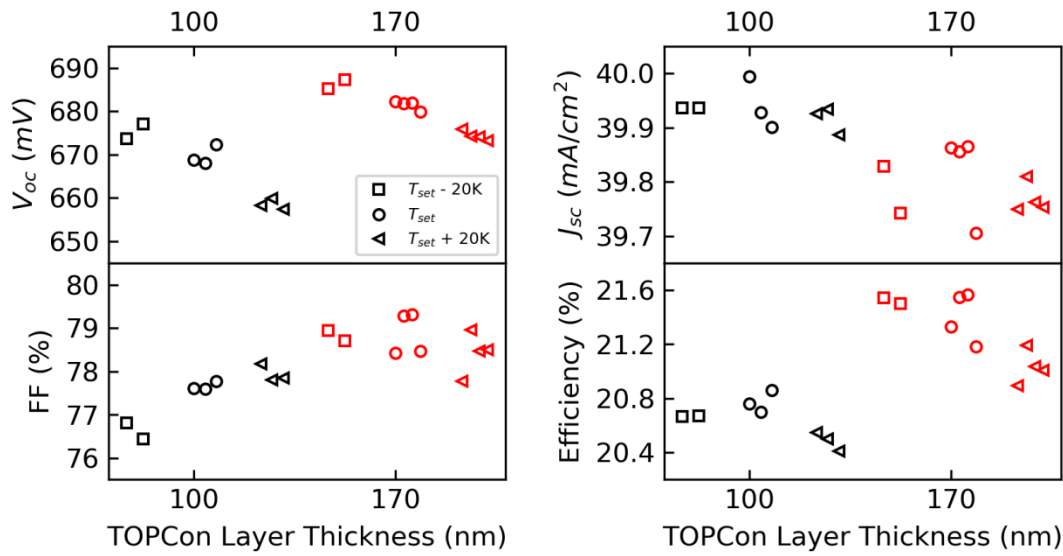


Figure 4: IV parameters of TOPCon solar cells featuring either 100 nm or 170 nm thick poly-Si layers. The different symbols refer to the different set firing temperatures.

3.3 Solar Cell Results

The measured IV parameters of TOPCon solar cells featuring 100 nm or 170 nm thick poly-Si layers are depicted in Fig. 4. Please note that above described process optimization was not implemented into the process sequence of these cells. As a result, iV_{oc} values of about 700 mV were measured on non-metallized solar cell precursors. In short, the cells featuring 170 nm poly-Si showed significantly higher V_{oc} and FF values but only marginally lower J_{sc} values than those cells featuring 100 nm poly-Si. Hence, the former group achieved a maximum efficiency of 21.6% at the lowest firing temperature.

In the following the cells will be analyzed in more detail with respect to V_{oc} and FF losses. As mentioned above, a V_{oc} limit of ~ 700 mV was imposed by non-optimal surface passivation. At the lowest firing temperature, the gap between iV_{oc} and V_{oc} was about 15 mV and 25 mV for cells featuring 170 nm and 100 nm poly-Si, respectively. The corresponding range of $J_{0,met}$ values at the rear contact was calculated by application of the one-diode model using the input parameters reported in Sec. 3.2. Fig. 5 displays a calculated V_{oc} - $J_{0,met}$ curve. Since the input parameters have a given uncertainty (as shown in the legend of Fig. 5), the upper and lower bounds were calculated by error propagation. For 170 nm poly-Si $J_{0,met,rear}$ took a value of about 530 ± 140 fA/cm², while a three times higher $J_{0,met,rear}$ value was obtained for 100 nm poly-Si. Hence, the benefit of a thicker poly-Si layer, which suppresses recombination at the metal contacts more effectively, is clearly visible.

The cells with 170 nm thick poly-Si layer also showed higher FF values than the cells featuring only 100 nm poly-Si. The main drivers for this are the substantially higher pseudo FF (pFF) values which are depicted in Fig. 6 together with the cells series resistance (R_s). The cells featuring 170 nm poly-Si showed pFF values of up to 84%. Interestingly, pFF deteriorated strongly with increasing firing temperature. On the other hand, pFF values of less than 83%, which deviate by more than 2% from the calculated ideal FF (FF_0), were

obtained on cells featuring 100 nm poly-Si. These rather low pFF values are due to non-ideal recombination losses, which are likely induced by spiking of the metal contacts. Moreover, R_s decreases with higher firing temperature which can be attributed to improved contact formation at both front and rear.

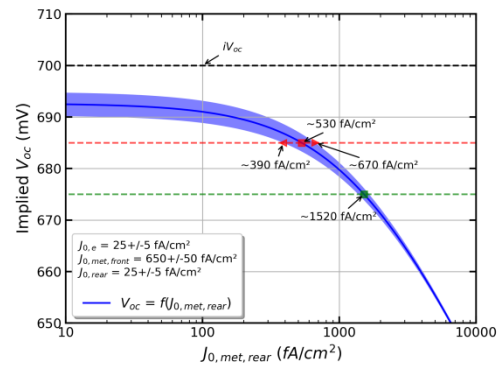


Figure 5: V_{oc} loss analysis based on 1-diode model.

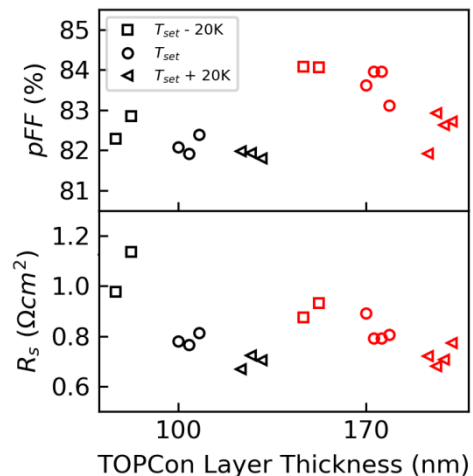


Figure 6: pFF and R_s values of TOPCon cells.

4 IMPROVED CELL TECHNOLOGY

The first cells were limited by non-optimal surface passivation, additional recombination losses at the metal contacts, and a rather high series resistance. One main contribution to R_S was the contact resistivity at the metal/TOPCon interface which took a value of 4-7 m Ω cm². One effective means to tackle this issue is to raise the poly-Si doping level. The resulting contact resistivity values are shown in Fig. 7. Contact resistivity values of about 1 m Ω cm² could be obtained by using a "very high" doping level of $N_{\text{poly-Si}} > 1 \times 10^{20}$ cm⁻³. It should be noted that such high doping level does not interfere with the surface passivation of TOPCon as the tunnel oxide is an effective diffusion barrier.

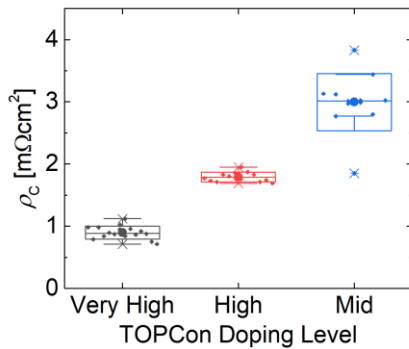


Figure 7: Contact resistivity as a function of the doping level of the poly-Si layer.

Another solar cell batch implementing more heavily-doped TOPCon structures was designed. Due to some process improvements an iV_{oc} of ~ 710 mV was measured on non-metallized solar cell precursors after firing thereby increasing V_{oc} to > 690 mV. Moreover, the reduction in rear contact resistivity yielded a gain in FF by more than 1%_{obs}. The best cell, which was measured at Fraunhofer ISE Callab, achieved an efficiency of 22.5%. The IV-parameters of the best cell are listed in Table I.

Table I: IV parameters of best cell independently confirmed by Fraunhofer ISE Callab.

	V_{oc} [mV]	FF [%]	J_{sc} [mA/cm ²]	η [%]
Best	691.2	80.7	40.4	22.5

5 SUMMARY AND OUTLOOK

It was demonstrated that a centrotherm cPLASMA PECVD tool can be used to deposit even thick TOPCon layers without blistering and that these TOPCon structures enable excellent surface passivation after low-temperature hydrogenation. Furthermore, a lower level of surface passivation was observed after firing unless certain adapted processes were applied.

The loss analysis of the first cells revealed a limitation in V_{oc} due to non-optimal surface passivation as well as additional recombination losses induced by the metal contacts at both sides. It was observed that $J_{0,met,rear}$ could be reduced by about 65% (estimated using the one-diode model) by employing a 170 nm thick poly-Si layer. After applying some process improvements as outlined in Section 4, another cell batch yielded a 22.5%-efficient solar cell.

Future work is dedicated to further minimizing

recombination losses. By optimizing surface passivation schemes, a high implied V_{oc} of 717 mV was already obtained on non-metallized solar cell precursors. Therefore, more emphasis will be put on improving contact formation so that both high V_{oc} and pFF (thereby raising FF) values can be realized on solar cell level.

6 ACKNOWLEDGEMENTS

The authors would like to thank Rainer Neubauer, Toni Leimenstoll, Felix Schätzle, Philipp Barth, Karin Zimmermann, Harald Steidl, Eleni Miethig, Leonard Kraus, Timo Wentzel, and many more colleagues for their support with processing.

This work was funded by the German Federal Ministry for Economic Affairs and Energy under contract numbers 0325877D (PEPPER) and 0324145 (PV-BAT400).

Some graphs were created using Python and the packages matplotlib [12], numpy [13], and uncertainties [14].

7 REFERENCES

- [1] F. Haase *et al.*, "Laser contact openings for local poly-Si-metal contacts enabling 26.1%-efficient POLO-IBC solar cells," *Sol. Energy Mater. Sol. Cells*, vol. 186, pp. 184–193, 2018.
- [2] A. Richter *et al.*, "n-Type Si solar cells with passivating electron contact: Identifying sources for efficiency limitations by wafer thickness and resistivity variation," *Solar Energy Materials and Solar Cells*, vol. 173, pp. 96–105, 2017.
- [3] F. Feldmann, M. Bivour, C. Reichel, M. Hermle, and S. W. Glunz, "Passivated rear contacts for high-efficiency n-type Si solar cells providing high interface passivation quality and excellent transport characteristics," *Sol Energ Mat Sol C*, vol. 120, no. Part A, pp. 270–274, 2014.
- [4] M. K. Stodolny *et al.*, "n-Type polysilicon passivating contact for industrial bifacial n-type solar cells," *Sol Energ Mat Sol C*.
- [5] N. Nandakumar *et al.*, "Approaching 23% with large- area monoPoly cells using screen- printed and fired rear passivating contacts fabricated by inline PECVD," *Prog Photovolt Res Appl*, vol. 15, no. 1, p. 41, 2018.
- [6] Y. Chen *et al.*, "Mass production of industrial tunnel oxide passivated contacts (i- TOPCon) silicon solar cells with average efficiency over 23% and modules over 345 W," *Progress in Photovoltaics: Research and Applications*, vol. 41, p. 46, 2019.
- [7] P. Padhamnath *et al.*, "Metal contact recombination in monoPoly™ solar cells with screen-printed & fire-through contacts," *Sol Energ Mat Sol C*, vol. 192, pp. 109–116, 2019.
- [8] M. K. Stodolny *et al.*, "Novel schemes of P+ polysi hydrogenation implemented in industrial 6" bifacial front-and-rear passivating contacts solar cells," *International Conference EU PVSEC for Photovoltaic Research, 24-28 September 2018, Brussels, Belgium, 1-4*, vol. 2018.

- [9] B. Steinhauser, J.-I. Polzin, F. Feldmann, M. Hermle, and S. W. Glunz, "Excellent Surface Passivation Quality on Crystalline Silicon Using Industrial-Scale Direct-Plasma TOPCon Deposition Technology," *Sol. RRL*, vol. 2, no. 7, p. 1800068, 2018.
- [10] D. Herrmann *et al.*, "Challenges for the Quantification of Metal Induced Recombination Losses,"
- [11] S. Werner, E. Lohmüller, A. Wolf, and F. Clement, "Extending the limits of screen-printed metallization of phosphorus- and boron-doped surfaces," *Sol. Energy Mater. Sol. Cells*, vol. 158, pp. 37–42, 2016.
- [12] J. D. Hunter, "Matplotlib: A 2D Graphics Environment," *Comput. Sci. Eng.*, vol. 9, no. 3, pp. 90–95, 2007.
- [13] S. van der Walt, S. C. Colbert, and G. Varoquaux, "The NumPy Array: A Structure for Efficient Numerical Computation," *Comput. Sci. Eng.*, vol. 13, no. 2, pp. 22–30, 2011.
- [14] Eric O. Lebigot, *Uncertainties: a Python package for calculations with uncertainties*.